

Intramolecular Charge Transfer in Dual Fluorescent 4-(Dialkylamino)benzonitriles. Reaction Efficiency Enhancement by Increasing the Size of the Amino and Benzonitrile Subunits by Alkyl Substituents

Yurii V. Il'ichev, Wolfgang Kühnle, and Klaas A. Zachariasse*

Max-Planck-Institut für biophysikalische Chemie, Spektroskopie und Photochemische Kinetik, D-37070 Göttingen, Germany

Received: December 4, 1997; In Final Form: February 26, 1998

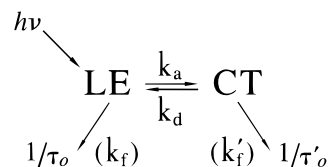
The intramolecular charge transfer (ICT) reaction from the locally excited state (LE) to the charge transfer state (CT) in the singlet excited state is investigated for the dual fluorescent 4-(dialkylamino)benzonitriles DRABN and 4-dialkylamino-2,6-dimethyl-benzonitriles RDB (R = methyl, ethyl, *n*-propyl) in toluene as a function of temperature by photostationary and time-resolved experiments. The efficiency of the ICT reaction, as expressed by the CT/LE fluorescence quantum yield ratio $\Phi'(\text{CT})/\Phi(\text{LE})$, is enhanced by the increase in the size of the dialkylamino group as well as by the presence of the two extra methyls in the phenyl ring. This increase is mainly brought about by slowing down the thermal back reaction (k_d) due to a larger activation energy E_d or a smaller preexponential factor k_d^0 , respectively. The free enthalpy change ΔG becomes more negative (~ 6 kJ/mol) for 4-(diethylamino)benzonitrile (DEABN) and 4-(di(*n*-propyl)amino)benzonitrile (DPrABN) as compared with 4-(dimethylamino)benzonitrile (DMABN) and also for the 4-dialkylamino-2,6-dimethylbenzonitriles EDB (ethyl) and PrDB (*n*-propyl) relative to MDB (methyl). The ΔG is about 2 kJ/mol more negative for RDB than for DRABN. In both series DRABN and RDB, the ICT stabilization enthalpy, $-\Delta H$, increases from R = methyl to *n*-propyl. The increase in the ICT rate constant k_a for the pairs DEABN/DMABN and EDB/MDB is primarily caused by a larger preexponential factor k_a^0 counteracted but not reversed by a likewise larger activation energy E_a . For the dependence of the energy $E(\text{CT})$ of the CT state on the difference between the redox potentials of the dialkylamino and benzonitrile moieties in DRABN and RDB a substantially smaller correlation coefficient (0.29) is found than the value of 1.0 expected for the TICT model, showing that the amino and benzonitrile groups in the CT state are not electronically decoupled. The energy δE_{rep} of the Franck–Condon ground state reached upon CT emission decreases with increasing size of the dialkylamino group in DRABN and RDB.

Introduction

4-(Dimethylamino)benzonitrile (DMABN) has over the years become the favorite example of a dual fluorescent molecule.^{1–3} Since the discovery that this molecule emits from two different intramolecular singlet excited states,³ a locally excited state LE and a charge transfer state CT, several mechanisms have been published to explain this phenomenon.^{1,3–6} The original hypothesis put forward by Lippert in 1959 was based on a solvent polarity induced reversal of the two directly populated lowest excited states S_1 and S_2 . Although it was pointed out that a small energy gap $\Delta E(S_1, S_2)$ was essential for the appearance of the dual emission, the molecular configuration of the two emitting states was not discussed.³ Alternative reaction mechanisms, proposed later, specifically address the molecular structure of the CT state.⁴ This structure and also the dynamics and the exact pathway of the LE \rightarrow CT reaction (Scheme 1), however, have not been completely clarified.

In Scheme 1, k_a and k_d are the rate constants of the forward and backward intramolecular charge transfer (ICT) reaction, respectively. τ_0 (LE) and τ_0' (CT) are the fluorescence lifetimes. The radiative rate constants k_f (LE) and k_f' (CT) have also been indicated. In the “twisted intramolecular charge transfer” (TICT) model, a 90° twist of the dimethylamino group with respect to the phenyl ring was considered to have occurred in the CT state of DMABN.¹ The dimethylamino group was

SCHEME 1

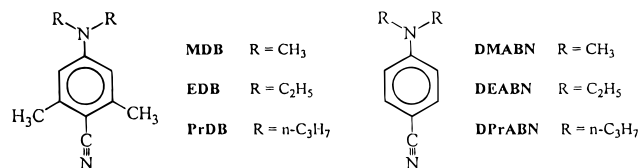


thereby assumed to be electronically decoupled from the rest of the molecule: the “principle of minimum overlap”.^{1d} Recently,^{5–7} evidence has been presented that the amino and benzonitrile moieties in a series of dual fluorescent 4-aminobenzonitriles are in fact not decoupled in the CT state. It has been shown that the configurational change of the amino nitrogen from pyramidal toward planar is an important reaction coordinate in the ICT reaction of these molecules and no evidence was found supporting the importance of a rotation of the amino group.^{6–9} In the “planar intramolecular charge transfer” (PICT) model based on these results, it is assumed that the relaxed CT state has an essentially planarized structure, with a less pyramidal amino nitrogen atom and different bond lengths than in the LE state, resulting in a larger dipole moment.^{10,11}

Because experimental methods to determine the molecular structure of excited states such as LE and CT in solution are not readily available, the reasoning leading to the TICT and PICT models just discussed is of an indirect nature. The TICT

hypothesis was based on the photophysical behavior of two kinds of model compounds, in which either the rotation of the amino group was blocked (supposed to mimic the LE state) or this group was pretwisted in the ground state by one or two methyl groups in ortho position, which was intended to be a model for the CT state.^{1,3} The PICT model in its turn was thought to find support from the strong decrease of the ICT efficiency with ring size in a series of 4-aminobenzonitriles in which the amino group is part of an eight- to three-membered heterocyclic ring.^{5–9} The increase of the ICT rate constant k_a with the length of the alkyl groups (methyl to *n*-butyl)^{2,9a,12,13} in the 4-(dialkylamino)benzonitriles also leads to the conclusion that a rotation of the dialkylamino group is not likely to be the determining factor in the formation of the CT state. In addition, it has been found that DMABN and 4-(diethylamino)benzonitrile (DEABN), for example, are dual fluorescent in ethanol glasses below the glass transition point,¹⁴ which provides evidence against the occurrence of a large amplitude motion during the ICT reaction of these molecules.

In the three 4-dialkylamino-2,6-dimethyl-benzonitriles MDB (methyl), EDB (ethyl) and PrDB (*n*-propyl), with methyl substituents on both sides of the cyano group, the CT/LE fluorescence quantum yield ratio $\Phi'(CT)/\Phi(LE)$ in toluene at 25 °C increases with alkyl chain length. Furthermore, under the same conditions, this ratio is larger for MDB than for DMABN.^{6,7} These results show that the efficiency of the ICT reaction in the 4-aminobenzonitriles becomes larger upon increasing the size of the amino group as well as of the benzonitrile moiety. Although the introduction of, for example,



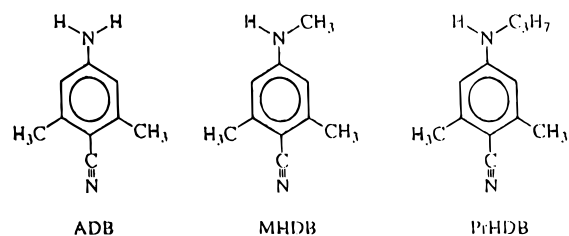
the two methyl groups in MDB indeed increases the size of the benzonitrile group as compared with DMABN, it should be realized that the presence of these substituents has additional consequences, like reducing the electron affinity of the benzonitrile moiety^{5–7} and leading to a decrease in the energy gap $\Delta E(S_1, S_2)$, as seen from the absorption spectra and the LE emission band.^{6,7} The introduction of additional substituents in molecules designed to act as model compounds can lead to changes different from those being envisaged. This is especially of importance when vibronic coupling between two close-lying excited states governs the photophysics, as has been proposed in the case of DMABN.^{5–9}

In the present paper, an investigation is presented of the kinetic and thermodynamic parameters for the ICT reaction in the series MDB–PrDB, abbreviated as RDB (R = methyl, ethyl, *n*-propyl), and in the group DMABN to 4-(di(*n*-propyl)amino)-benzonitrile (DPrABN), named DRABN.

Experimental Section

Solutes and Solvents. The compounds DMABN (Aldrich) and DEABN (K&K) were obtained commercially. 4-(Methylamino)benzonitrile (MABN) and DPrABN were synthesized as described before.⁶ MDB (mp, 90 °C), EDB (mp, 85.5 °C), and PrDB (liquid) were made by alkylation of 4-amino-2,6-dimethylbenzonitrile (ADB) with the corresponding alkyl iodide using a procedure described previously.¹⁰ Also formed during this reaction are the monomethylaminobenzonitriles 4-methylamino-2,6-dimethyl-benzonitrile (MHDB; mp, 115 °C), 4-(ethylamino)-

2,6-dimethyl-benzonitrile (EHDB; mp, 91.0 °C), and 4-(*n*-propyl)amino-2,6-dimethyl-benzonitrile (PrHDB; mp, 75 °C). These compounds are separated from the dialkylamino derivatives by chromatography over Al₂O₃ with cyclohexane/CHCl₃ (1:1). ADB was obtained from a reaction between 4-bromo-3,5-dimethylaniline (BDA) and CuCN in 2-pyrrolidinone by stirring the solution for 4 days at 135 °C. To synthesize BDA, 3,5-dimethylaniline (Aldrich) was converted with acetyl chloride to 3,5-dimethylacetanilide. This anilide was brominated in glacial acetic acid and finally treated with aqueous HCl. All compounds used in the fluorescence measurements were purified by HPLC. The solvent toluene (Merck; Uvasol) was refluxed



over potassium, just prior to use. *n*-Pentane (Merck; Uvasol) was used as received. The solutions for the fluorescence experiments were freed from oxygen by bubbling with nitrogen (15 min) or were deaerated by the freeze–pump–thaw method (five cycles). Solute concentrations were $\sim 4 \times 10^{-5}$ M.

Fluorescence Experiments. The fluorescence spectra were measured with a quantum-corrected Shimadzu 5000PC spectrophotometer. Fluorescence quantum yields were determined with quinine sulfate in 1.0 N H₂SO₄ as a standard ($\Phi = 0.546$ at 25 °C).¹⁵ The nanosecond time-resolved single-photon counting (SPC) measurements listed in Table 1 were carried out with an apparatus described previously.¹⁶ The decay times were determined at wavelengths where only fluorescence of either the LE (~ 340 nm) or the CT state (~ 470 nm) occurs. The picosecond fluorescence decays were obtained employing a system consisting of an argon ion laser (Coherent, Innova 100–10), a dye laser (Coherent 702–1CD; Rhodamine 6G), and a frequency doubler (LiIO₃, 297 nm).⁶ Alternatively, a mode-locked titanium-sapphire laser (Coherent, MIRA 900-F) pumped by an argon ion laser (Coherent, Innova 415) was used. The fluorescence and scatter records were detected with a Hamamatsu R2809U-07 or R3809U MCP photomultiplier (-3300 or -3100 V). The instrument response function has a width of ~ 30 ps at the excitation wavelength. The analysis of the fluorescence decays was carried out as reported earlier by using modulating functions, extended by global analysis.^{17,18}

Results and Discussion

Absorption Spectra and Energy Gap between S_1 and S_2 . The absorption spectra of ADB and its derivatives PrHDB and PrDB in *n*-pentane at 25 °C are shown in Figure 1a. With ADB, the relatively weak and slightly structured S_1 band between 280 and 310 nm is clearly separated from the stronger structureless S_2 absorption with a maximum around 265 nm. A similar behavior has been reported for 4-aminobenzonitrile (ABN), MABN, and DMABN.⁸ The energy gap $\Delta E(S_1, S_2)$ between S_1 and S_2 is smaller for PrHDB and, in the case of PrDB, the two bands strongly overlap, the vibrational structure of S_1 being still visible on the long-wavelength slope of the absorption spectrum (Figure 1a). With PrDB in toluene, this slope is completely smooth, indicating that $\Delta E(S_1, S_2)$ has become smaller than in *n*-pentane.

TABLE 1: Spectroscopic Data for 4-(Dialkylamino)benzonnitriles in Toluene at 25 °C

parameter	MDB	EDB	PrDB	MHDB	DMABN	DEABN	DPrABN	MABN
$E(\text{LE})$ [cm^{-1}] ^a	31350	31050	30900	(32000) ^b	31070	30880	30670	(31600) ^b
$h\nu^{\text{max}}(\text{LE})$ [cm^{-1}]	28840	28840	28800	29700	28560	28500	28500	29380
$h\nu^{\text{max}}(\text{CT})$ [cm^{-1}]	24760	24700	25160	—	24420	24560	24750	—
$h\nu^{\text{max}}(\text{abs})$ [cm^{-1}] ^c	33330	33000	32900	(35300) ^b	33800	33430	33330	(34800) ^b
$\Delta(1/2)$ [cm^{-1}] ^d	4400	4100	4100	—	4200	4000	4000	—
$h\nu^{\text{max}}(\text{abs}) - E(\text{LE})$ [cm^{-1}]	1980	1950	2000	(3300) ^b	2730	2550	2660	(3200) ^b
ϵ [$1 \text{ M}^{-1} \text{ cm}^{-1}$] ^e	26400	27900	27800	22400	26600	31100	30000	26100
$\Phi'(\text{CT})/\Phi(\text{LE})$	0.27	2.88	4.82	0.0	0.12	1.76	3.51	0.0
$\Phi(\text{LE}) + \Phi'(\text{CT})$	0.105	0.048	0.062	—	0.143	0.055	0.059	—
$\Phi(\text{LE})$	0.083	0.012	0.011	0.18	0.127	0.020	0.013	0.26
$\Phi'(\text{CT})$	0.022	0.036	0.051	0.0	0.016	0.035	0.046	0.0
$\Delta H(\text{SB})$ [kJ mol^{-1}]	-10.9	-11.1	-13.3	—	-7.2	-9.2	-11.2	—
$E_a(\text{SB})$ [kJ/mol]	- <i>f</i>	13.5	13.0	—	- <i>f</i>	14.7	12.7	—
$E_d(\text{SB})$ [kJ/mol]	- <i>f</i>	24.6	26.3	—	- <i>f</i>	23.9	23.9	—
$T_{\text{cr}}(\text{SB})$ [$^{\circ}\text{C}$]	- <i>f</i>	-40	-31	—	- <i>f</i>	-49	-42	—
k_f'/k_f (eq 5)	0.30	0.27	0.47	—	0.33	0.26	0.50	—
k_f [10^7 s^{-1}]	7.0	7.0	5.5	6.8 ^g	5.7	6.2	4.0	7.1 ^g
k_f' [10^7 s^{-1}]	2.1	1.9	2.6	—	1.9	1.6	2.0	—

^a Energy of the crossing point of the overlapping absorption and fluorescence bands, equalized at their maximum. ^b Cannot be determined accurately because of overlap with toluene absorption. ^c Maximum of absorption band (Figure 1). ^d Spectral width at half maximum of the CT emission band at around -72 °C in toluene. ^e Extinction coefficient in *n*-heptane. ^f Cannot be determined as the LTL limit (eq 7, see text) occurs at temperatures below the melting point of toluene (-95 °C). ^g $k_f = \Phi(\text{LE})/\tau_0$ calculated with the fluorescence lifetime τ_0 of MHDB (2.68 ns) or MABN (3.60 ns) in toluene at 25 °C (see ref 37).

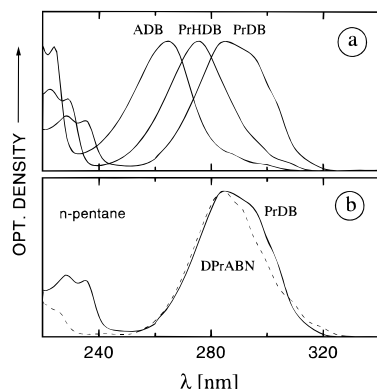


Figure 1. Absorption spectra in *n*-pentane at 25 °C of (a) 4-amino-2,6-dimethyl-benzonitrile (ADB), 4-(*n*-propyl)amino-2,6-dimethyl-benzonitrile (PrHDB), and 4-di(*n*-propyl)amino-2,6-dimethyl-benzonitrile (PrDB), and of (b) PrDB and 4-di(*n*-propyl)amino-benzonitrile (DPrABN).

In Figure 1b the absorption spectrum of PrDB in *n*-pentane is compared with that of DPrABN, showing that the lowest energy absorption (S_1) of PrDB is blue-shifted, whereas the main band (S_2) is red-shifted with respect to DPrABN (see Table 1). This result means that the energy gap $\Delta E(S_1, S_2)$ becomes smaller upon introduction of the two methyl groups next to the cyano substituent in PrDB. A similar observation is made for the two other pairs MDB/DMABN and EDB/DEABN (Table 1).

Fluorescence Spectra. RDB and DRABN. The fluorescence spectra of MDB, EDB, and PrDB in toluene at 25 °C are presented in Figure 2a. The fluorescence quantum yield ratio $\Phi'(\text{CT})/\Phi(\text{LE})$ becomes substantially larger with increasing length of the amino alkyl substituent from MDB to PrDB (Table 1). A similar enhancement is observed for the series DMABN, DEABN, and DPrABN in toluene^{6a} (see Figure 2b and Table 1) and in other solvents, such as cyclohexane, benzene, and diethyl ether.^{5,6b,10} From a comparison of Figure 2a and 2b it is seen that $\Phi'(\text{CT})/\Phi(\text{LE})$ is larger for MDB than for DMABN. The same holds for the two other pairs, EDB/DEABN and PrDB/DPrABN. These differences are observed over a large temperature range in toluene, from 90 to -70 °C.¹⁹ The data show that the overall efficiency²⁰ of the LE \rightarrow CT reaction is increased by lengthening the amino alkyl groups as well as by

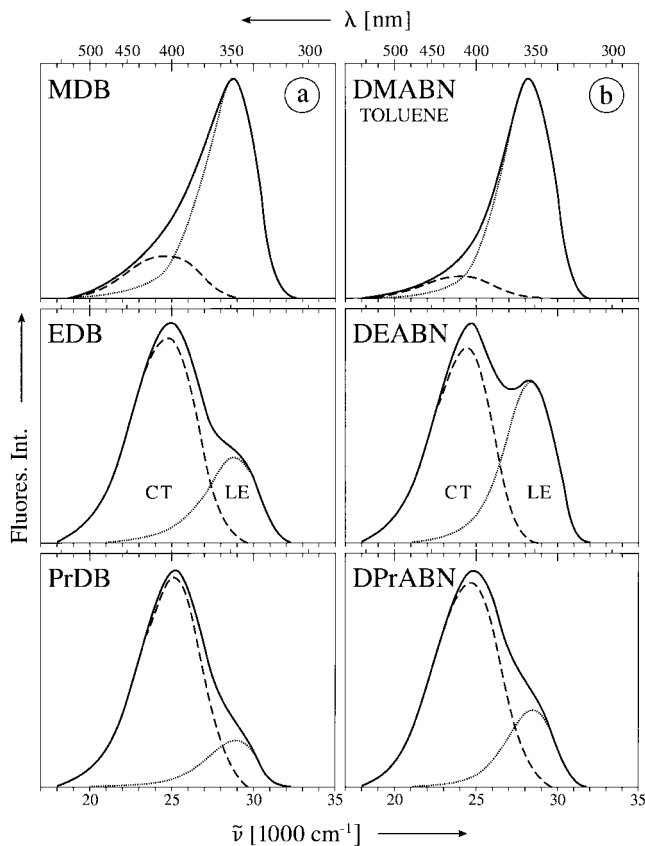


Figure 2. Fluorescence spectra of (a) the 4-dialkylamino-2,6-dimethyl-benzonitriles MDB (methyl), EDB (ethyl), PrDB (*n*-propyl), and (b) the 4-(dialkylamino)benzonnitriles DMABN (methyl), DEABN (ethyl), and DPrABN (*n*-propyl) at 25 °C in toluene. The CT and LE emission bands (see text; Scheme 1) were separated by taking the fluorescence spectrum of 4-methylamino-2,6-dimethyl-benzonitrile (MHDB) and 4-(methylamino)benzonitrile (MABN), respectively, to represent the emission of the LE state.

introducing the two methyls in the phenyl ring of the (dialkyl-amino)benzonnitriles. Note that both structural changes enlarge the size of either the amino or the benzonitrile subunits of these molecules.

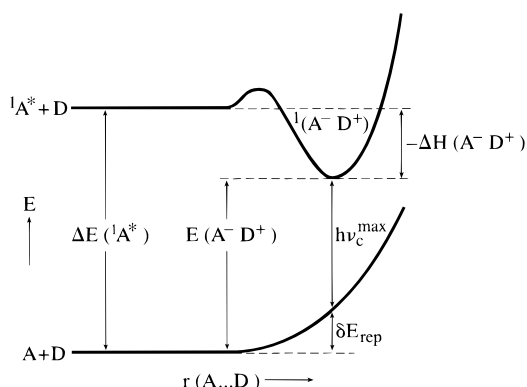


Figure 3. Schematic potential energy diagram for intermolecular exciplex formation and fluorescence. From an electron acceptor in the singlet excited state ${}^1A^*$ and an electron donor D , the exciplex ${}^1(A^-D^+)$ is formed with a stabilization enthalpy difference $-\Delta H(A^-D^+)$. The Franck–Condon (FC) state reached upon emission from the exciplex (energy of the CT emission maximum $h\nu_c^{\max}(\text{CT})$) is destabilized with respect to the equilibrated pair of ground-state molecules ($A + D$) by the repulsion energy δE_{rep} .

Energies of CT Emission Maxima in Terms of the Redox Potentials of D and A Subunits. The energy $h\nu_c^{\max}(\text{CT})$ of the CT emission maximum of dual fluorescent molecules such as DMABN has been discussed as a source of information on the structure of the CT state.²¹ In the TICT model, DMABN is treated as a D – A structure, in which the electron donor (D) and acceptor (A) parts are considered to be linked together by a single bond.²¹ The D and A groups are taken to be the dimethylamino and benzonitrile moieties, respectively.^{22,23} In the TICT model it is postulated, as already mentioned, that the D and A groups in the CT state of a dual fluorescent molecule such as DMABN are perpendicularly twisted relative to each other and therefore are electronically completely decoupled.^{1d} As a logical consequence of this model, it was then concluded that $h\nu_c^{\max}(\text{CT})$ should be linearly correlated with the difference $E(D/D^+) - E(A^-/A)$ of the redox potentials of the D and A subunits.²¹ The reasoning was based on the assumed analogy between the intramolecular CT state of a dual fluorescent molecule and an intermolecular exciplex (A^-D^+), in which the coupling between the A and D partners is weak. From the absence of dual fluorescence with dicyano derivatives of DMABN it has been concluded, however, that the appearance of dual emission cannot be predicted on the basis of the redox potentials of parts of the aminobenzonitriles.^{5–8}

Emission Maxima of Intermolecular Exciplexes and Redox Potentials. For intermolecular exciplexes (A^-D^+) with full charge transfer,²⁴ the exciplex energy $E(A^-D^+)$ is linearly correlated with the difference between the oxidation potential $E(D/D^+)$ of D and the reduction potential $E(A^-/A)$ of A (eq 1), meaning that in a series of exciplexes with a common donor, for example, the correlation coefficient between $E(A^-D^+)$ and $-E(A^-/A)$ is equal to unity.

$$E(A^-D^+) = E(D/D^+) - E(A^-/A) + C \quad (1)$$

The constant C in eq 1 depends on solvent polarity as well as on the specific molecular nature of the CT state and was experimentally determined to be equal to 0.15 eV in n -hexane: the Weller equation.^{24a,25} The energy of the exciplex emission maximum $h\nu_c^{\max}(\text{CT})$ is the difference between the energy $E(S_1)$ of the lowest singlet excited state ($\Delta E({}^1A^*)$ for the pair $A + D$ in Figure 3) and the sum of the exciplex stabilization enthalpy $-\Delta H$ (defined by eq 2) and the energy δE_{rep} of the Franck–

Condon (FC) state reached by CT fluorescence relative to the energy of the separate molecules A and D in their equilibrated ground states (see eq 3 and Figure 3).

$$-\Delta H = E(S_1) - E(A^-D^+) \quad (2)$$

$$h\nu_c^{\max}(\text{CT}) = E(S_1) - (-\Delta H + \delta E_{\text{rep}}) \quad (3)$$

By combining eqs 1–3, $h\nu_c^{\max}(\text{CT})$ can be expressed as a function of the redox potentials $E(D/D^+)$ and $E(A^-/A)$ and the ground-state repulsion energy δE_{rep} .

$$h\nu_c^{\max}(\text{CT}) = E(D/D^+) - E(A^-/A) - \delta E_{\text{rep}} + C \quad (4)$$

A linear correlation between $h\nu_c^{\max}(\text{CT})$ and the difference $E(D/D^+) - E(A^-/A)$ clearly will only exist when the ground state repulsion energy δE_{rep} is constant (eq 4), which is not a priori the case for exciplexes.⁵

Energies of CT Emission Maxima of RDB and DRABN.

The CT emission maxima of the 4-aminobenzonitriles, MDB–PrDB in toluene have energies of $\sim 25\,000\text{ cm}^{-1}$ (Figure 2a and Table 1), somewhat increasing from MDB to PrDB. A similar increase is found when going from DMABN to DPrABN (Figure 2b), with lower $h\nu_c^{\max}(\text{CT})$ values than for the former group of molecules.

The peak potential $E(D^+/D)$ of tri(n -propyl)amine is smaller (0.56 V versus SCE) than that of trimethylamine (0.83 V versus SCE),^{5,26,27} indicating that the former compound is a better electron donor. When δE_{rep} is constant, this difference in $E(D/D^+)$ should, within the context of the TICT model (see eq 4), lead to a substantial red-shift of $\sim 2200\text{ cm}^{-1}$ for $h\nu_c^{\max}(\text{CT})$ of, for example, PrDB relative to MDB.²⁷ This red-shift is clearly different from the blue-shift of 400 cm^{-1} observed here (Table 1). Also for DPrABN compared with DMABN, such a blue-shift (330 cm^{-1}) is found.

The presence of the two methyl groups on the phenyl ring of the molecules RDB, similarly leads to a small blue-shift ($\sim 300\text{ cm}^{-1}$) of the CT emission maximum compared with DRABN (Table 1). Although in this case the direction of the shift would, from the TICT point of view, be in accord with the more negative reduction potential (weaker electron accepting properties) of the dimethylbenzonitrile subunit (-2.48 V versus SCE) in these molecules relative to the benzonitrile group (-2.41 V versus SCE),²⁸ the extent of the spectral shift is only about half of that expected for this decrease when the linear correlation with the redox potentials (eq 4), in the case of constant δE_{rep} , would exist.^{28–30}

Aminobenzonitriles. No Linear Correlation of $h\nu_c^{\max}(\text{CT})$ with Redox Potentials. The energies $h\nu_c^{\max}(\text{CT})$ of a group of dual fluorescent 4-aminobenzonitriles and 4-amino-2,6-dimethyl-benzonitriles in diethyl ether and acetonitrile do not show a linear correlation with the redox potentials of their amino and benzonitrile subunits.^{5,6} The exceptionally large red-shift of the CT emission maximum observed for, for example, 1-(4-cyanophenyl)-4-methyl-piperazine (P6N) has been attributed to its large repulsion energy δE_{rep} .⁵

It is obvious therefore that the influence of the redox properties of the A and D subgroups in aminobenzonitriles on their fluorescence spectra and ICT behavior cannot be properly discussed on the basis of $h\nu_c^{\max}(\text{CT})$ data alone. To do so, the energy $E(\text{CT})$ of the CT state itself and hence its stabilization enthalpy $-\Delta H$ (eq 2a) must be known. These data can only

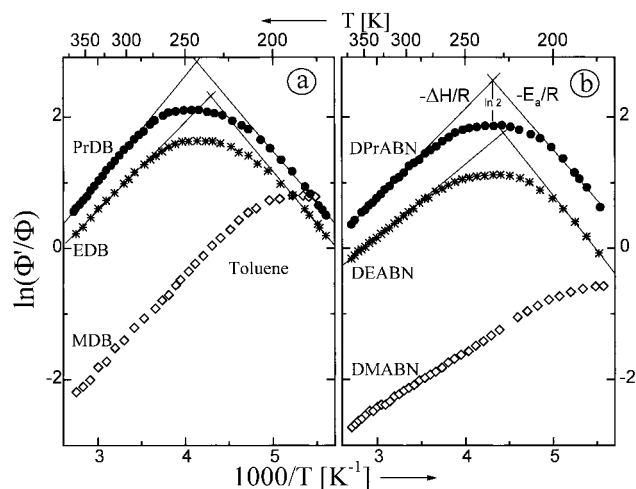


Figure 4. Plots of the natural logarithm of the CT/LE fluorescence quantum yield ratio $\Phi'(\text{CT})/\Phi(\text{LE})$ versus the reciprocal absolute temperature $1000/T$ (K), Stevens–Ban plots (eq 5), for the 4-dialkylamino-2,6-dimethyl-benzonitriles MDB (methyl), EDB (ethyl), and PrDB (*n*-propyl), and the 4-(dialkylamino)benzonitriles DMABN (methyl), DEABN (ethyl), and DPrABN (*n*-propyl) in toluene (see Figure 2). The HTL (eq 6) and the LTL slopes (eq 7) are drawn through the data points (see text).

be derived from time-resolved experiments,^{2,5–9} to be discussed in a later section.

$$-\Delta H = E(S_1) - E(\text{CT}) \quad (2a)$$

Fluorescence Spectra as a Function of Temperature. The ratio $\Phi'(\text{CT})/\Phi(\text{LE})$ was determined in toluene as a function of temperature for MDB, EDB, and PrDB (see Figure 4a), as well as for DMABN, DEABN, and DPrABN (see Figure 4b). The results are plotted as $\ln(\Phi'(\text{CT})/\Phi(\text{LE}))$ against the reciprocal absolute temperature: a so-called Stevens–Ban plot.³¹

For a reaction as described by Scheme 1, the following expression (eq 5) holds,

$$\frac{\Phi'(\text{CT})}{\Phi(\text{LE})} = \frac{k'_f [\text{CT}]}{k_f [\text{LE}]} = \frac{k'_f}{k_f} \frac{k_a}{k_d + 1/\tau'_0} \quad (5)$$

where [CT] and [LE] are, respectively, the photostationary concentrations of CT and LE.^{10,32}

Two limiting conditions can be distinguished, a high-temperature limit (HTL) with $k_d \gg 1/\tau'_0$, and a low-temperature limit (LTL) with $k_d \ll 1/\tau'_0$.³³

$$\frac{\Phi'(\text{CT})}{\Phi(\text{LE})} = \frac{k'_f k_a}{k_f k_d} \quad (\text{HTL}) \quad (6)$$

$$\frac{\Phi'(\text{CT})}{\Phi(\text{LE})} = \frac{k'_f}{k_f} k_a \tau'_0 \quad (\text{LTL}) \quad (7)$$

From the slope, $-\Delta H(\text{SB})/R$ (eq 6), of a Stevens–Ban plot under HTL conditions, the reaction enthalpy $-\Delta H$ can be determined, provided that k'_f/k_f does not depend on temperature. The activation energy E_a of the forward ICT reaction is obtained from the LTL slope $-E_a(\text{SB})/R$ (eq 7), when k'_f/k_f and τ'_0 are temperature independent. It is further tacitly assumed in this treatment that E_a and E_d , and hence $-\Delta H (= E_d - E_a)$, do not change with temperature (vide infra).^{34,35} The temperature at which the maximum value of $\Phi'(\text{CT})/\Phi(\text{LE})$ is reached (Figure 4), is related to the temperature T_{cr} at which the HTL and LTL lines intersect. This crossing is reached when $k_d = 1/\tau'_0$, independent of assumptions on the temperature dependence of k'_f/k_f or τ'_0 (see eqs 6 and 7). In a Stevens–Ban plot of a system governed by Scheme 1, the vertical distance between the HTL/LTL intersection and the experimental $\ln(\Phi'(\text{CT})/\Phi(\text{LE}))$ curve (eq 5) is equal to $\ln 2$, a useful diagnostic.^{2,33} The parameter T_{cr} , different from $\Delta H(\text{SB})$ and $E_a(\text{SB})$, does not depend on k'_f/k_f .

TABLE 2: Kinetic and Thermodynamic Data for 4-(Dialkylamino)benzonitriles in Toluene

parameter	T [°C]	MDB	EDB	PrDB	DMABN	DEABN	DPrABN
τ_1 [ns]		2.40	2.13	2.21	(3.10) ^a	2.60	2.76
τ_2 [ns]	+20	0.027	0.025	0.024	(0.016) ^a	0.020	0.018
A_{12}/A_{11} (eq 16)		0.57	12.1	17.2	(0.41) ^a	7.9	9.5
k_a [10^9 s ⁻¹]		(24) ^a	38	41	(18) ^a	44	50
k_d [10^9 s ⁻¹]	+20	(23) ^a	3.1	2.4	(45) ^a	5.6	5.3
τ'_0 [ns]		(2.0) ^a	2.0	2.1	(2.7) ^a	2.5	2.7
τ_1 [ns]		2.66	2.31	2.40	3.44	2.93	2.87
τ_2 [ns]	-20	0.049	0.047	0.040	0.042	0.041	0.032
A_{12}/A_{11} (eq 16)		2.2	31.7	59.2	0.92	16.7	22.4
k_a [10^9 s ⁻¹]		14	20	24	11	23	30
k_d [10^9 s ⁻¹]	-20	6.2	0.63	0.41	12	1.4	1.3
τ'_0 [ns]		2.4	2.3	2.4	3.1	2.9	2.8
ΔG [kJ/mol]	+20	-0.03	-6.4	-6.3	+2.2	-5.0	-5.2
ΔG [kJ/mol]	-20	-1.8	-7.5	-7.8	+0.3	-6.0	-6.6
E_a [kJ/mol]		6.0	8.5	6.9	7.8	11.0	9.4
E_d [kJ/mol]		19.1	23.4	24.0	19.4	23.3	24.4
k_a^0 [10^{12} s ⁻¹]		0.28	1.3	0.66	0.45	4.2	2.5
k_d^0 [10^{12} s ⁻¹]		60	41	56	129	83	136
T_{cr} [°C]		-83	-28	-29	-94	-48	-46
ΔH [kJ/mol]		-13.1	-14.9	-17.1	-11.6	-12.3	-15.0
$\Delta H(\text{SB})$ [kJ/mol] ^b		-10.9	-11.1	-13.3	-7.2	-9.2	-11.2
ΔS [J/K·mol] ^c		-44.6	-29.1	-36.9	-47.2	-24.9	-33.3
δE_{rep} [kJ/mol] ^d		65.7	61.1	51.6	68.0	63.3	55.8
$E(\text{CT})$ [kJ/mol] ^e		362	357	353	360	357	352
E_f [kJ/mol] ^f		—	1.9	4.2	4.1	2.9	4.9
$A(f)$ ^f		—	0.59	2.06	1.68	0.65	3.38

^a Extrapolated from lower temperatures (Figure 6). ^b From Stevens–Ban plots (Figure 4); see Table 1. ^c $\Delta S = R \ln(k_a^0/k_d^0)$. ^d Ground state repulsion energy; see eq 3 and Figure 3. ^e $E(\text{CT}) = E(\text{LE}) + \Delta H$; see Table 1. ^f $k'_f/k_f = A(f) \exp(-E_f/RT)$ (eq 5).

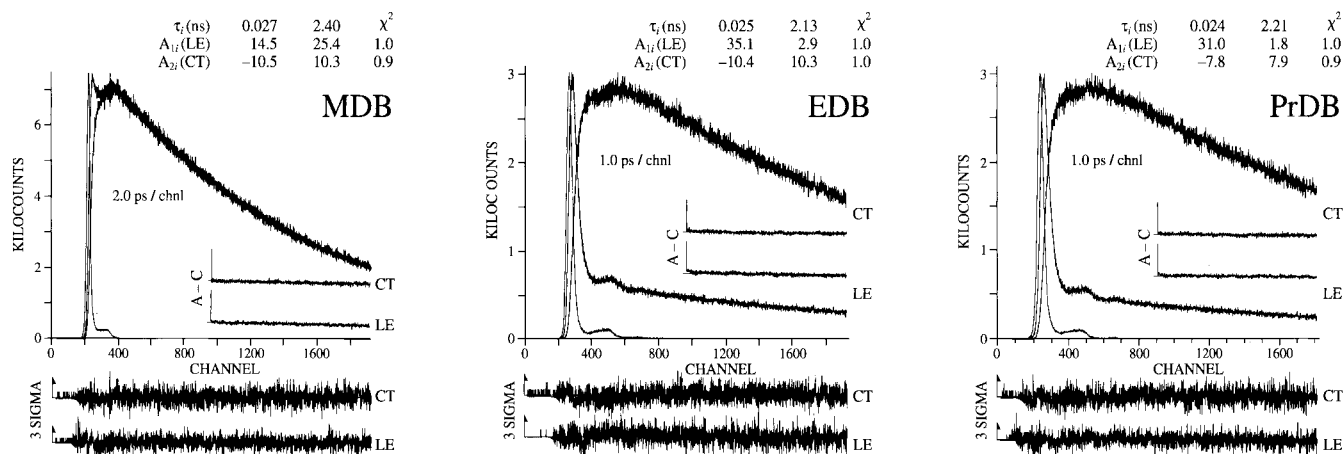


Figure 5. Initially excited LE and subsequently formed CT fluorescence response functions of the 4-dialkylamino-2,6-dimethyl-benzonitriles MDB (methyl), EDB (ethyl), and PrDB (*n*-propyl) in toluene at 20 °C. The LE and CT decays are analyzed simultaneously (global analysis). The decay times (τ_1 , τ_2) and their preexponential factors A_{1i} (LE) and A_{2i} (CT) are given (see eqs 11 and 12). The shortest decay time τ_2 is listed first. The weighted deviations, expressed in σ (expected deviations), the autocorrelation functions A-C, and the values for χ^2 are also indicated.

Activation Energies E_a and E_d and Stevens-Ban Plots.

The slope $-\Delta H(\text{SB})/R$ of the HTL line in a Stevens-Ban plot (eq 6) is in fact determined by three activation energies (eq 8). As a simple approximation, the temperature dependence of k_f'/k_f is expressed in Arrhenius form: $k_f'/k_f = A(f)e^{-E_f/RT}$.

$$-\Delta H(\text{SB})/R = -E_a(\text{SB}) + E_d(\text{SB}) = -E_d/R + E_d/R - E_f/R = -\Delta H/R - E_f/R \quad (8)$$

Similarly, the slope of the LTL line in a Stevens-Ban plot (eq 7) is given by eq 9

$$-E_a(\text{SB})/R = -E_d/R - E_f/R + E_f/R \quad (9)$$

where E_τ is the formal activation energy of the reciprocal CT lifetime $1/\tau_o'$ analyzed in Arrhenius form. As τ_o' only slightly depends on temperature for the present molecules under the LTL conditions (Figures 7b and 8),² the term E_f/R in eq 9 is neglected. By subtraction of eqs 8 and 9 it then follows that $E_d(\text{SB})$ is equal to E_d (eq 10).

$$E_d(\text{SB}) = -\Delta H(\text{SB}) + E_a(\text{SB}) = E_d - E_\tau \approx E_d \quad (10)$$

Some data for the ICT reaction of the 4-aminobenzonitriles can already be obtained from the photostationary data presented in Figures 4a and 4b, such as the relative values of T_{cr} , $\Delta H(\text{SB})$ (eq 8), $E_a(\text{SB})$ (eq 9), and E_d (eq 10); see Table 1.

Data from Stevens-Ban Plots. A reliable piece of information to be obtained from a Stevens-Ban plot, is the temperature T_{cr} at which the HTL and LTL lines in the $\Phi'(\text{CT})/\Phi(\text{LE})$ plots (eqs 6 and 7) cross (see Figure 4). At this temperature, k_d is equal to $1/\tau_o'$, as already discussed. The value of T_{cr} is clearly lower for MDB than for EDB (-40 °C) and PrDB (-31 °C). This value cannot be determined for MDB because $\Phi'(\text{CT})/\Phi(\text{LE})$ has its maximum near the melting point of the solvent, which means (see previous section) that the equality $k_d = 1/\tau_o'$ is reached at a much lower temperature for MDB than for EDB and PrDB. When the three compounds have an approximately equal CT lifetime τ_o' , which is the case (Table 2, below), it then follows that k_d is considerably larger for MDB than for EDB and PrDB. For DMABN in toluene it likewise can be concluded, from the plots in Figure 4b, that the condition $k_d = 1/\tau_o'$ is reached at a much lower temperature² than for DEABN (-49 °C) and DPrABN (-42 °C), see Table 1, again

indicating that at given temperature k_d is larger for DMABN than for the two other molecules.

The presence of the two additional ring methyl groups in MDB compared with DMABN leads to an increase in $-\Delta H(\text{SB})$, from 7 to 11 kJ/mol (Table 1). A similar conclusion is reached for the two other pairs EDB/DEABN and PrDB/DPrABN. For the two groups of aminobenzonitriles RDB and DRABN, $-\Delta H(\text{SB})$ increases when R changes from methyl to *n*-propyl. The activation energies E_d , determined from the difference between the LTL and HTL slopes (eq 10), are similar for the pairs EDB/DEABN and PrDB/DPrABN. Data for E_d of MDB and DMABN are not available from the Stevens-Ban plots because the LTL region of these molecules is below the melting point of toluene (see Figure 4).²

Although $\Phi'(\text{CT})/\Phi(\text{LE})$ is larger for MDB than for DMABN over the entire temperature range covered in Figure 4, it cannot be concluded that this increase is caused by k_a because $\Phi'(\text{CT})/\Phi(\text{LE})$ under HTL conditions is determined by the ratio k_d/k_d (eq 6).²⁰ The same conclusion holds for EDB/DEABN and PrDB/DPrABN. Time-resolved measurements, to be presented in the next section, are required to determine the ICT rate constants and thermodynamic data separately.

Time-Resolved Measurements. *CT and LE Fluorescence Decays.* The fluorescence decay (LE) and rise/decay curves (CT) of MDB, EDB, and PrDB in toluene at ~20 °C are presented in Figure 5. These decays were analyzed by the method of global analysis.^{2,17} At this temperature, both curves are double exponential (Table 2), which means that two excited state species are taking part in the ICT reaction, in accordance with Scheme 1.

For the LE and CT fluorescence response functions, the following well-known³² expressions (eqs 11-17) hold, with the decay times τ_i and the amplitudes A_{ij} ($i, j = 1, 2$).

$$i_{\text{LE}}(t) = A_{11}e^{-t/\tau_1} + A_{12}e^{-t/\tau_2} \quad (11)$$

$$i_{\text{CT}}(t) = A_{21}e^{-t/\tau_1} + A_{22}e^{-t/\tau_2} \quad (12)$$

$$1/\tau_{1,2} = \frac{1}{2}\{(X + Y) \mp [(X - Y)^2 + 4k_a k_d]^{1/2}\} \quad (13)$$

with

$$X = k_a + 1/\tau_o \quad (14)$$

and

$$Y = k_d + 1/\tau'_0 \quad (15)$$

$$A = \frac{A_{12}}{A_{11}} = \frac{(X - 1/\tau_1)}{(1/\tau_2 - X)} \quad (16)$$

$$\frac{A_{22}}{A_{21}} = -1 \quad (17)$$

Inspection of the fluorescence decay curves reveals that the shortest time τ_2 (Figure 5) decreases only slightly from MDB (27 ps) to PrDB (24 ps). The LE amplitude ratio A_{12}/A_{11} , however, is much larger for EDB (12.1) and PrDB (17.2) than for MDB (0.57). The increase in A signifies that k_a/k_d becomes more than 20 times larger when the dimethylamino substituent in MDB is replaced by a diethylamino group.³⁶ The ratio A increases further when going from EDB to PrDB, but to a smaller extent (factor 1.4). Similar results are obtained for DMABN–DPrABN in toluene and also in diethyl ether.^{6,9b} For DRABN in toluene, A and hence k_a/k_d is smaller than for the corresponding RDB compound (Table 2).^{5–10,12,13} Note that the CT amplitude ratio $-A_{22}/A_{21}$ is equal to unity (eq 17, Figure 5), which means that the CT state cannot be reached directly by excitation of the molecules in the ground state S_0 .^{2,5–10}

ICT Rate Constants at 20 °C. From the decay parameters τ_1 , τ_2 , and A and the fluorescence lifetime τ_o of a model compound,^{2,10,37} such as MHDB in the case of RDB or MABN for DRABN, the rate constants k_a and k_d as well as the CT lifetime τ'_0 can be determined with eqs 13–16. The results are listed in Table 2.

It is seen that k_a at 20 °C increases from MDB ($24 \times 10^9 \text{ s}^{-1}$) to EDB ($38 \times 10^9 \text{ s}^{-1}$) and PrDB ($41 \times 10^9 \text{ s}^{-1}$). The backward ICT reaction rate constant k_d is considerably smaller for EDB ($3.1 \times 10^9 \text{ s}^{-1}$) and PrDB ($2.4 \times 10^9 \text{ s}^{-1}$) than for MDB ($23 \times 10^9 \text{ s}^{-1}$). These changes in k_a and k_d result in a more negative ΔG for EDB and PrDB (–6 kJ/mol) than for MDB (0 kJ/mol).

For the three molecules DRABN in toluene at 20 °C, k_a likewise increases with increasing length of the dialkylamino groups (Table 2): DMABN ($18 \times 10^9 \text{ s}^{-1}$), DEABN ($44 \times 10^9 \text{ s}^{-1}$), and DPrABN ($50 \times 10^9 \text{ s}^{-1}$). The rate constant k_d of the dimethylamino compound DMABN ($45 \times 10^9 \text{ s}^{-1}$) at this temperature is again much larger than that of DEABN ($5.6 \times 10^9 \text{ s}^{-1}$) and that of DPrABN ($5.3 \times 10^9 \text{ s}^{-1}$). The change in ΔG with the size of the dialkylamino substituent from 2 kJ/mol for DMABN to –5 kJ/mol (DEABN and DPrABN) is similar to that found for the compounds RDB. At other temperatures, the same pattern is observed (see the data for –20 °C in Table 2 and the complete temperature dependence in Figure 6). A comparison of the data for MDB and DMABN in Table 2 reveals that k_d is a factor of ~2 smaller for the former molecule. The changes in k_a are relatively minor. Similar results are obtained for EDB/DEABN and PrDB/DPrABN, with a more negative ΔG for RDB than for DRABN.

Temperature Dependence of LE and CT Fluorescence Decays. The increase in k_a and the decrease in k_d observed when comparing the two series MDB–PrDB and DMABN–DPrABN (Table 2) can in principle be caused by the preexponential factor k_i^o as well as by the activation energy E_i appearing in the Arrhenius expression $k_i^o e^{-E_i/RT}$ which is assumed to be valid for these rate constants. This separate influence of k_i^o and E_i is investigated here by measuring the LE and CT

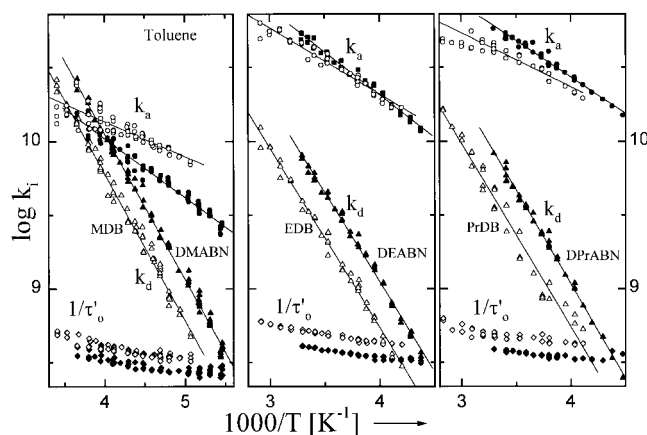


Figure 6. Arrhenius plot of the ICT rate constants k_a and k_d and the reciprocal CT lifetime $1/\tau'_0$ (Scheme 1) for the 4-dialkylamino-2,6-dimethylbenzonnitriles MDB (methyl), EDB (ethyl), and PrDB (*n*-propyl), and the 4-(dialkylamino)benzonnitriles DMABN (methyl), DEABN (ethyl), and DPrABN (*n*-propyl) in toluene. From the slopes of the straight lines fitted through the data points E_a and E_d are obtained (see Table 2).

fluorescence decays of the 4-aminobenzonnitriles as a function of temperature.

The LE and, at several temperatures, the CT fluorescence response functions of MDB, EDB, and PrDB in toluene were measured from 20 °C or higher temperatures (EDB and PrDB) to the melting point of the solvent (–95 °C). These fluorescence decays were found to be double exponential (see Figure 7) down to –80 °C (MDB) and –40 °C (EDB, PrDB). At lower temperatures, the decay curves become triple exponential.^{38–41} Similar observations were made for DEABN and DPrABN,¹³ whereas the fluorescence decays of DMABN in toluene can adequately be fitted to two exponentials down to –95 °C.^{2,41} The data analysis based on Scheme 1, requiring double exponential decay curves,² was therefore limited to the higher temperature ranges.

As an example, the decay times τ_1 and τ_2 and also their amplitude ratio A (eqs 11 and 12) of DEABN in toluene from 30 to –45 °C are plotted in Figure 8a. The rate constants k_a and k_d as well as the reciprocal CT lifetime $1/\tau'_0$ resulting from these decay parameters (eqs 13–16) are presented as Arrhenius plots in Figure 8b. From the slopes of the straight line through the data points for k_a and k_d , the activation energies E_a and E_d and hence the CT stabilization enthalpy $-\Delta H (=E_a - E_d)$ are determined. Time-resolved fluorescence experiments were likewise carried out for DMABN,² DPrABN, and MDB–PrDB in toluene as a function of temperature (see Figure 8 and Table 2).

The reciprocal CT lifetimes $1/\tau'_0$ are considerably smaller than k_a and k_d (Figures 6 and 8b), over the temperature range in which the fluorescence decays are double exponential. This result means that under these conditions, the ICT reaction kinetics is primarily governed by k_a and k_d . The ratio $\Phi'(\text{CT})/\Phi(\text{LE})$ is, in addition, influenced by k_i^o/k_i (eq 5).

Counteracting Effects of E_a and k_a^o . The increase in k_a observed at all temperatures in toluene, when going from MDB to EDB and PrDB (Figure 6), is primarily caused by a substantially larger preexponential factor k_a^o for the two latter molecules (see Table 2): $1.3 \times 10^{12} \text{ s}^{-1}$ (EDB) and $0.66 \times 10^{12} \text{ s}^{-1}$ (PrDB) compared with $0.28 \times 10^{12} \text{ s}^{-1}$ (MDB). This effect is counteracted but not reversed, however, by a simultaneous increase of the activation energy E_a for EDB (8.5 kJ/mol) and PrDB (6.9 kJ/mol) relative to MDB (6.0 kJ/mol).

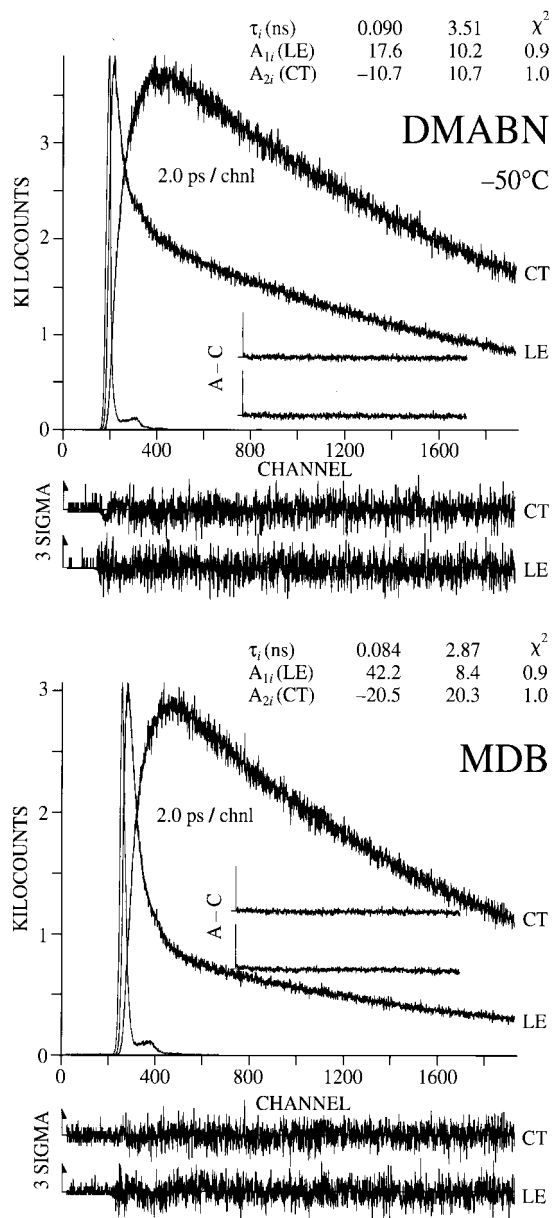


Figure 7. Initially excited LE and subsequently formed CT fluorescence response functions of 4-(dimethylamino)benzonitrile (DMABN) and 4-dimethylamino-2,6-dimethyl-benzonitrile (MDB) in toluene at $-50\text{ }^\circ\text{C}$. The LE and CT decays are analyzed simultaneously (global analysis). See the caption of Figure 5.

In the series DRABN, k_a similarly increases with increasing size of the dialkylamino group, especially from DMABN to DEABN (Table 2). Also here, these changes are mainly caused by the preexponential factor k_a^0 : $0.45 \times 10^{12}\text{ s}^{-1}$ (MDB) compared with $4.2 \times 10^{12}\text{ s}^{-1}$ (EDB) and $2.5 \times 10^{12}\text{ s}^{-1}$ (PrDB). These changes are again counteracted by an increase in E_a : 7.8 kJ/mol (DMABN) compared with 11.0 kJ/mol (DEABN) and 9.4 kJ/mol (DPrABN).

Influence of k_a and k_d on $\Phi'(\text{CT})/\Phi(\text{LE})$. The CT/LE quantum yield ratio $\Phi'(\text{CT})/\Phi(\text{LE})$ in the fluorescence spectra is determined by k_a and k_d , together with τ_o' (eq 5). It can now be understood why $\Phi'(\text{CT})/\Phi(\text{LE})$ at $25\text{ }^\circ\text{C}$ in toluene is more than 10 times larger (see Table 1) for EDB (2.88) and PrDB (4.82) than for MDB (0.27) as well as at least 15 times larger for DEABN (1.76) and DPrABN (3.51) than for DMABN (0.12). This increase, which is found over the entire temperature range studied (Figure 4), is in the first place caused by a smaller

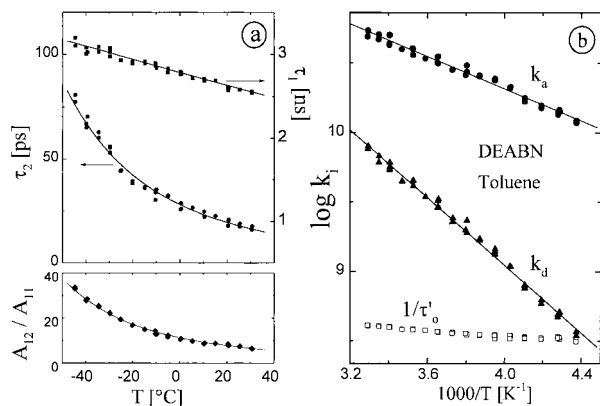


Figure 8. (a) The decay times τ_1 and τ_2 and also the amplitude ratio A_{12}/A_{11} (eqs 11, 12, and 16) of 4-(diethylamino)benzonitrile (DEABN) in toluene from 30 to $-50\text{ }^\circ\text{C}$. (b) Arrhenius plot of the ICT rate constants k_a and k_d and the reciprocal CT lifetime $1/\tau_o'$ (Scheme 1) of DEABN in toluene. From the slopes of the straight lines fitted through the data points E_a and E_d are obtained (see Table 2).

k_d and to some extent also by a larger k_a for the former compounds relative to MDB and DMABN (Table 2 and Figure 6). Part of the increase in $\Phi'(\text{CT})/\Phi(\text{LE})$ discussed here is due to k_f'/k_f (eq 5), which is larger for PrDB than for MDB as well as for DPrABN compared with DMABN (see Table 1 and a later section). Also shown in Table 1 is that $\Phi'(\text{CT})/\Phi(\text{LE})$ is two times larger for MDB (0.27) than for DMABN (0.12). A similar situation holds for EDB/DEABN and PrDB/DPrABN, with a decrease in E_a , an increase in $-\Delta H$, an unchanged E_d , and smaller prefactors k_a^0 and k_d^0 as a consequence of the introduction of the two methyls in the phenyl ring (Table 2).

E_a and the Size of the Dialkylamino and Benzonitrile Groups. The activation energy E_a becomes larger when going from MDB (6.0 kJ/mol) to EDB (8.5 kJ/mol). A similar increase, also mentioned previously, is observed for DEABN (11.0 kJ/mol) relative to DMABN (7.8 kJ/mol). This change might at first sight be attributed to the larger size of the diethyl- compared with the dimethylamino group, which could be expected to lead to an energetically less favorable ICT reaction pathway for EDB and DEABN when a large amplitude configurational change would occur during the ICT reaction. However, E_a of PrDB (6.9 kJ/mol) is smaller than that of EDB and for DPrABN (9.4 kJ/mol), a similar decrease in E_a is observed relative to DEABN. For the molecules RDB a smaller E_a is obtained than for their DRABN counterparts, although the size of the benzonitrile subunit is larger in the former molecules. These results lead to the conclusion that the magnitude of E_a and the overall ICT kinetics of DRABN and RDB cannot be related to simple structural or configurational properties of the aminobenzonitriles, such as the size of the dialkylamino or benzonitrile subgroups in these molecules.

Correlation of $E(\text{CT})$ with Redox Potentials of the Amino and Benzonitrile Subgroups. The ICT stabilization enthalpy $-\Delta H$ of the aminobenzonitriles increases with increasing size of the dialkylamino group from 13 to 17 kJ/mol for RDB and from 12 to 15 kJ/mol for DRABN (see Table 2). From these data, the energy $E(\text{CT})$ of the CT state can be calculated (eq 2a; see Table 2). For MDB, $E(\text{CT})$ (362 kJ/mol) is only slightly larger than that of DMABN (360 kJ/mol). Similar minor differences occur for the pairs EDB/DEABN and PrDB/DPrABN. Within the groups RDB and DRABN, $E(\text{CT})$ likewise somewhat decreases with increasing size of the dialkylamino group; for example, from 362 kJ/mol for MDB to 357 kJ/mol in the case of EDB.

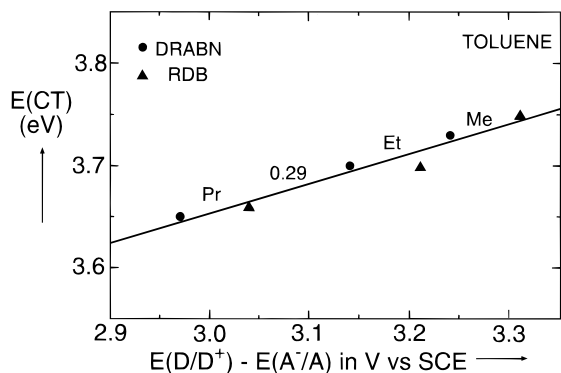


Figure 9. Plot of the energy $E(\text{CT})$ for the CT state of the 4-dialkylamino-2,6-dimethyl-benzonitriles MDB (methyl), EDB (ethyl), and PrDB (*n*-propyl), and the 4-(dialkylamino)benzonitriles DMABN (methyl), DEABN (ethyl), and DPrABN (*n*-propyl) in toluene against the difference between the oxidation potential $E(D/D^+)$ and the reduction potential $E(A^-/A)$ of the corresponding trialkylamines (D) and benzonitriles (A). D and A are taken as the electron donor and acceptor moieties, respectively, in which the aminobenzonitriles are partitioned in the hypothetical structure $D-A$. The correlation coefficient is equal to 0.29 (see eq 1a and text).

In the TICT model, the D subunits in RDB and DRABN can be represented by a trialkylamine, whereas for the A moieties, either 2,4,6-trimethylbenzonitrile or 4-methylbenzonitrile can be taken. The dependence of $E(\text{CT})$ on the difference between the oxidation potential $E(D/D^+)$ of the trialkylamines²⁷ and the reduction potential $E(A^-/A)$ of the benzonitriles²⁸ (eq 1a) leads to a correlation coefficient (slope) of 0.29 for RDB and DRABN; see Figure 9.

$$E(\text{CT}) = E(D/D^+) - E(A^-/A) + C \quad (1a)$$

This result shows that $E(\text{CT})$ for the two groups of compounds is not linearly correlated (eq 1a) with the difference $E(D/D^+) - E(A^-/A)$ between the redox potentials of the electron donor (D) and acceptor (A) parts in which these molecules are commonly partitioned in the TICT approach, in clear contrast with the requirements of the this model. Although the correlation coefficient is much smaller than 1.0, the data do in fact show that the energy $E(\text{CT})$ of the D/A -substituted molecules undergoes the influence of the electron donor and acceptor properties of the D and A moieties. The molecular nature of the substituents determines the extent of the CT interactions in the various excited singlet states S_n . This is the reason that ICT does, for example, not occur with unsubstituted anilines or with 4-(methoxy)anilines and with 4-(dimethylamino)-phenylacetylene,⁴² but that its appearance in the anilines requires relatively strong electron acceptor substituents such as a cyano or ester group.^{1,3,5}

The ICT behavior of the present aminobenzonitriles RDB and DRABN can therefore not be understood on the basis of the TICT model, in which the redox potentials of the decoupled amino and benzonitrile moieties are supposed to determine the energy of the CT state. These redox potentials are hence by themselves not a useful criterion in predicting whether ICT and dual fluorescence will occur or not.^{5,6}

Temperature Dependence of Radiative Rates k'_f , k_f , and k'_f/k_f . The temperature dependence of the CT/LE ratio of the radiative rate constants k'_f/k_f (eq 5) as well as of the individual rate constants k'_f and k_f was determined for DMABN in toluene from 25 to -90 °C (Figure 10), by measuring $\Phi'(\text{CT})/\Phi(\text{LE})$ and also the quantum yields $\Phi'(\text{CT})$ and $\Phi(\text{LE})$ as a function of temperature.⁴³ The data were corrected for the change in optical density of the solution by way of the temperature

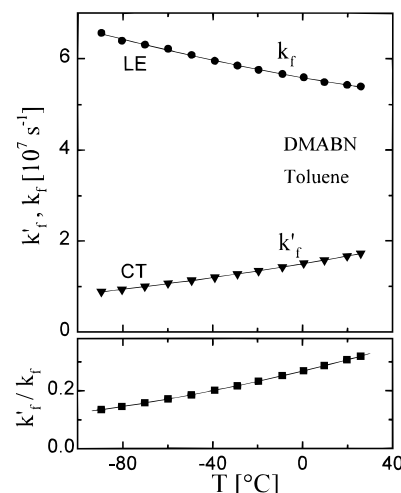


Figure 10. Plots of (upper) the CT/LE ratio of radiative rate constants k'_f/k_f and (lower) the individual radiative rate constants k'_f and k_f (eq 5) for 4-(dimethylamino)benzonitrile (DMABN) in toluene as a function of temperature.

dependence of the solvent density. It appears that k'_f/k_f becomes smaller when the temperature is lowered. This change is brought about by two factors: a decrease of k'_f and a simultaneous increase of k_f (Figure 10). A similar temperature dependence of k'_f/k_f , k'_f , and k_f is obtained for DEABN, DPrABN, and MDB-PrDB. For MABN and MHDB, which only show LE fluorescence,^{2,6} k_f in toluene likewise becomes larger upon cooling, which is attributed to the increase of the solvent refractive index n .^{32,34,35,44}

The observation that k'_f does not approach the value of zero in toluene at -94 °C means that the amino and benzonitrile groups of the CT state are not in a condition of minimum overlap, as postulated in the TICT model.⁴⁵ This results is in line with the conclusion of the nonzero coupling between these groups (PICT model),^{5,7} based on the correlation coefficient of 0.29 for the difference between the redox potentials of the A and D moieties and the energy of the CT state $E(\text{CT})$, as discussed in the previous section.⁵ The temperature dependence of k'_f/k_f can formally be expressed in the Arrhenius form $k'_f/k_f = A(f)e^{-E_f/RT}$ see eqs 8 and 9. The data for $A(f)$ and E_f are listed in Table 2. The largest values for E_f (and also for k'_f/k_f and $A(f)$) are found for DPrABN (4.9 kJ/mol) and PrDB (4.2 kJ/mol). Information on E_f is needed when the results from photostationary (Stevens-Ban plots, eqs 8–10) and time-resolved measurements are compared.

Comparison of Data From Time-Resolved Experiments and Stevens-Ban Plots. A comparison of the data for RDB and DRABN in Tables 1 and 2 reveals that ΔH and E_a derived from time-resolved experiments in toluene are larger than $\Delta H(\text{SB})$ and $E_a(\text{SB})$ obtained from Stevens-Ban plots. For E_d , about the same values are found by the two methods. These observations can be explained by looking at eqs 8–10. The differences $(\Delta H(\text{SB}) - \Delta H)$ and $(E_a(\text{SB}) - E_a)$ are equal to E_f , with values between 2 and 5 kJ/mol (Table 2), whereas E_d is expected not to differ from $E_d(\text{SB})$ because the CT lifetime τ'_0 of the present molecules is independent of temperature under LTL conditions (eq 10; see Figure 6 and 8b).

From a comparison of the $\Phi'(\text{CT})/\Phi(\text{LE})$ plots (Figure 4 and Table 1) and simulations of these plots with the data from the time-resolved experiments (Table 2), it follows that E_a is indeed smaller for DMABN than for DEABN and DPrABN. For MDB, a similar conclusion can be drawn with respect to EDB and PrDB (see Table 2). It is therefore concluded that the

observed (Table 2) substantial increase in the preexponential factor k_a^0 from $0.3 \times 10^{12} \text{ s}^{-1}$ for MDB to $\sim 1 \times 10^{12} \text{ s}^{-1}$ for EDB and PrDB and from $0.5 \times 10^{12} \text{ s}^{-1}$ for DMABN to $4.2 \times 10^{12} \text{ s}^{-1}$ for DEABN and $2.5 \times 10^{12} \text{ s}^{-1}$ for DPrABN is real. This is an important conclusion because E_a and k_a^0 are mutually related. In general, when in an Arrhenius expression $k_a = k_a^0 e^{-E_a/RT}$ the experimentally obtained activation energy E_a is for some reason overestimated, this error will be compensated by a correspondingly too large value for k_a^0 and vice versa.

Influence of Temperature Dependent Solvent Polarity on E_a , E_d , and ΔH . The polarity of a solvent generally increases upon cooling.^{34,35} Therefore, measurements of E_a , E_d , and ΔH from $\Phi'(\text{CT})/\Phi(\text{LE})$ and also from time-resolved experiments do not take place under constant polarity conditions. For molecules such as RDB and DRABN, with a larger dipole moment for the CT than for the LE state,¹⁰ $-\Delta H$ will increase upon cooling. Also E_a and E_d decrease with increasing solvent polarity^{13,46} and hence upon lowering the temperature, in contrast to the assumption of constant activation energies underlying eqs 8–10. The E_a values derived here from the measurements over a temperature range from 25 to -40°C (Table 2), will therefore be smaller than the value applicable at the higher temperature. The same is the case for E_d and ΔH . The increase in ϵ , n_D , and $f - 1/2f'$ for toluene, from 2.37, 1.4940, and 0.126 at 25°C to 2.56, 1.5310, and 0.136 at -40°C , is relatively small, however.³⁵ This comparison means that the values in Table 2 are not influenced to a large extent by the temperature dependence of the solvent polarity.

The Magnitude of the CT Repulsion Energy δE_{rep} . The CT ground state repulsion energy δE_{rep} (eq 4) of the present (dialkylamino)benzonitriles decreases with increasing size of the dialkylamino group: from 66 kJ/mol (MDB) to 52 kJ/mol (PrDB) for RDB and from 68 kJ/mol (DMABN) to 56 kJ/mol (DPrABN) for DRABN (Table 2). Generally, the magnitude of δE_{rep} reflects the differences between the molecular configuration of the CT and the equilibrated ground state, as well as the different orientation of the solvent molecules around CT and S_0 caused by the increase in dipole moment, from 7 to 17 D during the ICT reaction for the DRABN compounds.¹⁰ Because the CT and S_0 dipole moments remain the same in this series,¹⁰ a change in solvent molecule orientation will not contribute to the observed decrease in δE_{rep} .

The changes in molecular configuration during the LE \rightarrow CT reaction may involve a decrease in pyramidal character of the amino nitrogen, which is considered to be an important reaction coordinate in this reaction,^{5–9} as well as differences in bond length caused by the increase in charge separation. This conclusion is drawn from crystal structure data, which show that for DEABN, the pyramidal character of the amino group is smaller than for DMABN.^{47–49} A variation in bond length has been found for the radical cation of *N,N,N',N'*-tetramethyl-*p*-phenylenediamine (TMPD) relative to the uncharged molecule.⁵⁰

Conclusion

The kinetic and thermodynamic parameters for the ICT reaction of two sets of three 4-(dialkylamino)benzonitriles DMABN–DPrABN and MDB–PrDB in toluene were investigated. The modifications in the structure of these molecules involve the change of the amino group from dimethyl- to di-(*n*-propyl)amino and the introduction of two methyl groups ortho to the cyano substituent in the phenyl ring. The efficiency of the ICT reaction is enhanced by both changes. This conclusion is deduced from the CT/LE fluorescence quantum yield ratio $\Phi'(\text{CT})/\Phi(\text{LE})$, which is determined by the forward (k_a) as well as by the backward (k_d) rate constants. In DRABN and RDB,

the effect on the ICT kinetics of replacing the dimethylamino by a diethylamino substituent is much larger than that caused by a further change to the di(*n*-propyl)amino group.

The rate constant k_a is larger for DEABN and DPrABN than for DMABN over the entire temperature range studied. This result is due to an increase in the preexponential factor k_a^0 , counteracted but not overruled by a simultaneous increase in the activation energy E_a . For EDB and PrDB compared with MDB, a similar result is observed. The change in the size of the dialkylamino group has a larger impact on k_d than on k_a , which results from an increase in the activation energy E_d , whereas the preexponential factors k_d^0 remain practically unchanged. In both sets DRABN and RDB, $-\Delta H$ increases with increasing size of the dialkylamino group. The presence of the two additional methyls in the series RDB leads to a smaller activation energy E_a and a larger ICT stabilization enthalpy $-\Delta H$ than for the corresponding DRABN molecule.

The influence of the structural changes in the aminobenzonitriles studied here on the ICT reaction is complex, as several effects occur simultaneously, such as changes in the energy gap $\Delta E(S_1, S_2)$ and in the size and electron donating ability of the amino nitrogen. Therefore, although the results presented here give kinetic reasons for the variation in the ICT efficiency, they do not provide simple answers to questions related to the molecular structure of the CT state.

The energy $E(\text{CT})$ depends on the difference between the redox potentials of the dialkylamino and benzonitrile moieties in the aminobenzonitriles, with a correlation coefficient of 0.29. This value is substantially smaller than the coefficient 1.0 to be expected when the TICT model would be valid, showing that the amino and benzonitrile groups are not electronically decoupled in the CT state of these molecules. Such a correlation cannot be investigated by using the CT emission maxima $h\nu^{\text{max}}(\text{CT})$ because the FC ground state repulsion energy δE_{rep} is not constant. It is found for DRABN as well as for RDB that δE_{rep} decreases with increasing size of the dialkylamino group.

Acknowledgment. The present investigations were supported in part by the Volkswagen Foundation (Project Intra- and Intermolecular Electron Transfer). Thanks are due to J. Fries and Dr. C. Seidel for measuring a series of reduction potentials. The valuable assistance of H. Lesche in the determination of the fluorescence quantum yields is gratefully acknowledged.

References and Notes

- (1) (a) Grabowski, Z. R.; Rotkiewicz, K.; Rubaszewska, W.; Kirkor-Kaminska, E. *Acta Phys. Pol.* **1978**, A54, 767. (b) Grabowski, Z.; Rotkiewicz, K.; Siemiarz, A.; Cowley, D. J.; Baumann, W. *Nouv. J. Chim.* **1979**, 3, 443. (c) Rettig, W. *Angew. Chem., Int. Ed. Engl.* **1986**, 25, 971. (d) Lippert, E.; Rettig, W.; Bonačić-Koutecký, V.; Heisel, F.; Miehé, J. A. *Adv. Chem. Phys.* **1987**, 68, 1.
- (2) Leinhos, U.; Kühnle, W.; Zachariasse, K. A. *J. Phys. Chem.* **1991**, 95, 2013.
- (3) (a) Lippert, E.; Lüder, W.; Boos H. In *Advances in Molecular Spectroscopy; European Conference on Molecular Spectroscopy, Bologna, Italy, 1959*; Mangini, A., Ed.; Pergamon: Oxford, 1962; p 443. (b) Lippert, E.; Lüder, W.; Moll, F.; Nagele, H.; Boos H.; Prigge, H.; Siebold-Blankenstein, I. *Angew. Chem.* **1961**, 73, 695. (c) Lippert, E. In *Luminescence of Organic and Inorganic Materials*; Kallmann, H. P., Spruch, G. M., Eds.; Wiley: New York, 1962; p 271. (d) Lippert, E. In *Organic Molecular Photophysics*; Birks, J., Ed.; Wiley: London, 1975; Vol. 2, p 1.
- (4) References to models for the dual fluorescence of DMABN reported in the literature are given in ref 2. The recent RICT model of Sobolewski and Domcke, introduced on the basis of theoretical calculations, is discussed in ref 42, where it is reported that an experimental verification of the predictions of this model could not be obtained.
- (5) von der Haar, Th.; Hebecker, A.; Il'ichev, Y.; Jiang, Y.-B.; Kühnle, W.; Zachariasse, K. A. *Recl. Trav. Chim. Pays-Bas.* **1995**, 114, 430.
- (6) (a) Zachariasse, K. A.; Grobys, M.; von der Haar, Th.; Hebecker, A.; Il'ichev, Yu. V.; Jiang, Y.-B.; Morawski, O.; Kühnle, W. *J. Photochem. Photobiol. A: Chem.* **1996**, 102, 59. (b) von der Haar, Th.; Hebecker, A.;

Il'ichev, Yu. V.; Kühnle, W.; Zachariasse, K. A. In *Fast Elementary Processes in Chemical and Biological Systems*, Lille, France, 1995, *AIP Conf. Proc.* **1996**, 364, 295.

(7) Zachariasse, K. A.; Grobys, M.; von der Haar, Th.; Hebecker, A.; Il'ichev, Yu. V.; Morawski, O.; Rückert, I.; Kühnle, W. *J. Photochem. Photobiol. A: Chem.* **1997**, 105, 373.

(8) Zachariasse, K. A.; von der Haar, Th.; Hebecker, A.; Leinhos, U.; Kühnle, W. *Pure Appl. Chem.* **1993**, 65, 1745.

(9) (a) Zachariasse, K. A.; von der Haar, Th.; Leinhos, U.; Kühnle, W. *J. Inf. Rec. Mats.* **1994**, 21, 501. (b) Zachariasse, K. A.; Grobys, M.; von der Haar, Th.; Hebecker, A.; Il'ichev, Yu. V.; Kühnle, W.; Morawski, O. *J. Inf. Recording* **1996**, 22, 553.

(10) Schuddeboom, W.; Jonker, S. A.; Warman, J. M.; Leinhos, U.; Kühnle, W.; Zachariasse, K. A. *J. Phys. Chem.* **1992**, 96, 10809.

(11) Baumann, W.; Bischof, H.; Fröhling, J.-C.; Brittinger, C.; Rettig, W.; Rotkiewicz, K. *J. Photochem. Photobiol. A: Chem.* **1992**, 64, 49.

(12) In the series of 4-(dialkylamino)benzonitriles DRABN (R = methyl to *n*-pentyl (DPABN) and *n*-decyl (DDABN)) in toluene, k_a increases from DMABN to DBABN, whereas k_a decreases upon further lengthening of the amino alkyl substituents.^{9a,13} For the CT/LE fluorescence quantum yield ratio $\Phi'(CT)/\Phi(LE)$, a similar dependence on alkyl chain length is observed.¹³ $\Phi'(CT)/\Phi(LE)$ increases from DMABN to DDABN in cyclohexane at 25 °C, whereas this ratio is slightly smaller for DDABN than for DPrABN in benzene and 1,4-dioxane at 25 °C.¹⁰

(13) Leinhos, U. Ph.D. Thesis, University Göttingen, Germany, 1991.

(14) Von der Haar, Th.; Il'ichev, Yu. V.; Zachariasse, K. A., unpublished results.

(15) Demas, J. N.; Crosby, G. A. *J. Phys. Chem.* **1971**, 75, 991.

(16) Zachariasse, K. A.; Duvencek, G.; Busse, R. *J. Am. Chem. Soc.* **1984**, 106, 1045.

(17) Striker, G. In *Deconvolution and Reconvolution of Analytical Signals*; Bouchy, M., Ed.; University Press: Nancy, France, 1982; p 329.

(18) Zachariasse, K. A.; Kühnle, W.; Leinhos, U.; Reynders, P.; Striker, G. *J. Phys. Chem.* **1991**, 95, 5476.

(19) The maximum in the plot of $\ln(\Phi'(CT)/\Phi(LE))$ versus $1000/T$ (K) occurs at much lower temperatures for MDB and DMABN than for their derivatives EDB/PrDB and DEABN/DPrABN; see Figure 4.

(20) The overall efficiency of an ICT reaction is defined here by the magnitude of the ratio $\Phi'(CT)/\Phi(LE)$ (eq 5). In the HTL limit (eq 6), this efficiency is determined by the ratio k_a/k_d , indicating that an increase in ICT efficiency does not automatically mean that k_a has become larger. The increase in efficiency can be caused either by an increase of k_a , a decrease of k_d , or a combination of both.

(21) (a) Grabowski, Z. R.; Dobkowski, J. *Pure Appl. Chem.* **1983**, 55, 245. (b) Dobkowski, J.; Herbich, J.; Waluk, J.; Koput, J.; Kühnle, W. *J. Lumin.* **1989**, 44, 149. (c) Dobkowski, J.; Grabowski, Z. R.; Jasny, J.; Zieliński, Z. *Acta Phys. Polon.* **1995**, 88A, 455.

(22) In 4-(dimethylamino)-4'-cyano-stilbene (DCS), different suggestions have been made to partition the molecule in *D* and *A* subunits. The dimethylamino as well as the dimethylamino groups were considered as the electron donor in discussions based on the TICT model (see ref 23 and the literature cited there).

(23) Il'ichev, Yu. V.; Kühnle, W.; Zachariasse, K. A. *Chem. Phys.* **1996**, 211, 441.

(24) (a) Weller, A. In *The Exciplex*, Gordon, M., Ware, W. R., Eds.; Academic: New York, 1975; p 23. (b) Beens, H.; Weller, A. *Acta Phys. Polon.* **1968**, 34, 593.

(25) (a) Weller, A. *Z. Phys. Chem.* **1982**, 133, 93. (b) Weller, A. *Z. Phys. Chem.* **1982**, 130, 129.

(26) (a) Lindsay Smith, J. R.; Masheder, D. *J. Chem. Soc., Perkin Trans. 2* **1977**, 47. (b) Mann, C. K. *Anal. Chem.* **1964**, 36, 2424.

(27) For the oxidation potential $E(D/D^+)$ of the trialkylamines, the following data are taken (versus SCE): 0.83 V (trimethylamine), 0.73 V (triethylamine), and 0.56 V (tri(*n*-propyl)amine); see ref 26. Using these data, an energy difference of -0.27 eV (2178 cm⁻¹, red-shift) would be expected for the CT emission maxima of the pairs MDB/PrDB and DMABN/DPrABN, when a linear correlation (eq 4) between $h\nu^{\max}(CT)$ and the redox potentials of the *A* and *D* subunits in the aminobenzonitriles would exist (see text).

(28) The reduction potentials $E(A^-/A)$ of 2,4,6-trimethylbenzotrile (TMBN), 4-methylbenzotrile (MBN), and benzotrile (BN) in dimethylformamide at 20 °C were remeasured: -2.48 V, -2.41 V, and -2.31 V versus SCE, respectively.²⁹ In earlier publications,^{5,6,30} the values of -2.47 V for TMBN and -2.34 V versus SCE for BN were used. From the difference in reduction potential between MBN and TMBN, an energy difference of 0.07 eV (565 cm⁻¹, blue-shift) would be expected for the CT emission maxima of in the series MDB-PrDB compared with those in DMABN-DPrABN, when a linear correlation (eq 4) between $h\nu^{\max}(CT)$ and the redox potentials of the *A* and *D* subunits in the aminobenzonitriles would exist (see text).

(29) (a) The reduction potentials of anthracene (-1.95 V versus SCE) and ferrocene (0.45 V versus SCE, 0.57 V versus Ag/AgCl, saturated in acetonitrile) were measured as standards in the same set of experiments;

Fries, J.; Seidel C., unpublished results. (b) Seidel, C. Ph.D. Thesis, University Heidelberg, Germany, 1992.

(30) (a) Zachariasse, K. A. Ph.D. Thesis, Free University, Amsterdam, The Netherlands, 1972. (b) Zachariasse, K. A. In *The Exciplex*; Gordon, M., Ware, W. R., Eds.; Academic: New York, 1975; p 275.

(31) Stevens, B.; Ban, M. I. *Trans. Faraday Soc.* **1964**, 60, 1515.

(32) Birks, J. B. *Photophysics of Aromatic Molecules*; Wiley: London, 1970.

(33) (a) Zachariasse, K. A.; Kühnle, W.; Weller, A. *Chem. Phys. Lett.* **1978**, 59, 375. (b) Zachariasse, K. A. *Trends Photochem. Photobiol.* **1994**, 3, 211.

(34) In general, the polarity of a solvent, determined by the dielectric constant ϵ and the refractive index n_D , increases with decreasing temperature. For toluene, $f - 1/2f$, ϵ , and n_D increase respectively from 0.119, 2.24, and 1.4626 at 81 °C to 0.147, 2.75, and 1.5629 at -94 °C.³⁵ The solvent polarity parameter $f - 1/2f$ is defined as $(\epsilon - 1)/(2\epsilon + 1) - 1/2(n^2 - 1)/(2n^2 + 1)$.¹⁰ As a consequence of this increase in polarity, the CT emission maximum $h\nu^{\max}(CT)$ of DMABN in toluene shifts to the red upon cooling, from $24\,480$ cm⁻¹ at 81 °C to $23\,120$ cm⁻¹ at -94 °C.¹⁴

(35) (a) *Landolt-Börnstein, Zahlenwerte und Funktionen*, Bd II/6, *Elektrische Eigenschaften I*, 6th edition; Hellwege, K. H., Hellwege, A. M., Eds.; Springer: Berlin, 1959. (b) Timmermans, J. *Physico-Chemical Constants of Pure Organic Compounds*, Vol. II; Elsevier: New York, 1965.

(36) With MDB and the other 4-(dialkylamino)benzonitriles (Figure 5) in toluene at 20 °C, the conditions $k_a, k_d \gg 1/\tau_0, 1/\tau_0'$, and $\tau_1 \gg \tau_2$ hold.^{2,5-10} Hence, $A_{12}/A_{11} = (X - 1/\tau_1)/(1/\tau_2 - X) \approx k_a/(k_a + k_d - k_a) = k_a/k_d$ (eq 16). This follows from eqs 13-15, giving $1/\tau_1 + 1/\tau_2 = k_a + k_d + 1/\tau_0 + 1/\tau_0'$, which reduces in the present situation to $1/\tau_2 \approx k_a + k_d$.

(37) The fluorescence lifetime τ_0 of MHDB is 2.79 ns at 20 °C and 3.47 ns at -20 °C. For MABN τ_0 is 3.65 ns at 20 °C and 3.87 ns at -20 °C.²

(38) The appearance of triple exponential fluorescence decays can be caused by the presence of three excited state species, such as in the case of 1,3-di(1-pyrenyl)propane with one monomer and two configurationally different intramolecular excimers.³⁹ With DEABN and the other aminobenzonitriles in toluene discussed here, two different LE states (*S*₁ and *S*₂) could be emissive next to the CT state.¹³ Also, in diethyl ether, triple exponential decays are observed with DEABN at low temperatures.¹⁴ It should be noted that the additional third decay time is considerably longer than the longitudinal dielectric relaxation time of toluene.^{2,40} The possible influence of dielectric solvent relaxation on the excited state behavior of DRABN and RDB in toluene will be discussed separately.

(39) Zachariasse, K. A.; Busse, R.; Duvencek, G.; Kühnle, W. *J. Photochem.* **1985**, 28, 237.

(40) Whiffen, D. H.; Thompson, H. W. *Faraday Discuss. Chem. Soc.* **1946**, 42A, 122.

(41) The quality (χ^2) of the double exponential fluorescence decays of DMABN in toluene somewhat deteriorates between -85 and -95 °C, although acceptable² fits are still obtained. This reduction in fit quality may indicate the onset of triple exponential decays for DMABN in this temperature region.

(42) Zachariasse, K. A.; Grobys, M.; Tauer, E. *Chem. Phys. Lett.* **1997**, 274, 372.

(43) For k_f and k_f' , the following equations hold (Scheme 1): $k_f = \Phi(LE)/(1/\tau_0 + 1/\tau_0' \cdot (k_a/(k_a + 1/\tau_0')))$ and $k_f' = \Phi'(CT)/(1/\tau_0' + 1/\tau_0 \cdot (k_d + 1/\tau_0)/k_a)$.

(44) The LE radiative rate k_f for MABN in toluene increases upon cooling, from 7.1×10^7 s⁻¹ at 25 °C to 9.7×10^7 s⁻¹ at -94 °C. For MHDB in toluene, k_f increases from 6.8×10^7 s⁻¹ at 25 °C to 9.0×10^7 s⁻¹ at -94 °C. Based on the relation of k_f with n^2 ,³² the increase in the refractive index n_D from 1.4940 at 25 °C to 1.5629 at -94 °C would lead to an expected 1.1-fold increase of k_f , which is somewhat smaller than the factor of 1.3 observed for both MABN and MHDB.

(45) Van der Auweraer, M.; Grabowski, Z.; Rettig, W. *J. Phys. Chem.* **1991**, 95, 2083.

(46) Hicks, J.; Vandersall, M.; Babarogic, Z.; Eissenthal, K. B. *Chem. Phys. Lett.* **1985**, 116, 18.

(47) In a DMABN crystal,⁴⁸ the pyramidal angle θ between the plane of the two carbons of the dimethylamino group and the phenyl ring is equal to 12° and, correspondingly, the sum of the angles ΣN° around the amino N is with 358.5° (at 253 K) smaller than the 360° for a planar (sp²) nitrogen atom. For DEABN, θ is smaller (6°) than for DMABN and ΣN° is close to 360°.⁴⁹

(48) Heine, A.; Herbst-Irmer, R.; Stalke, D.; Zachariasse, K. A. *Acta Crystallogr.* **1994**, B50, 363.

(49) von Bülow, R.; Stalke, D.; Zachariasse, K. A., unpublished results.

(50) (a) Ikemoto, I.; Katagiri, G.; Nishimura, S.; Yakushi, K.; Kuroda, H. *Acta Crystallogr.* **1979**, B35, 2264. (b) De Boer, J. L.; Vos, A. *Acta Crystallogr.* **1972**, B28, 835.